Antiferromagnetic, charge-transfer, and pairing correlations in the three-band Hubbard model

R. T. Scalettar
Department of Physics, University of California, Davis, California 95616

D. J. Scalapino and R. L. Sugar
Department of Physics, University of California, Santa Barbara, California 93106

S. R. White
Department of Physics, University of California, Irvine, California 92717

(Received 16 May 1990)

The CuO_2 sheets common to the superconducting cuprates are believed to be characterized by a charge-transfer gap in their insulating antiferromagnetic state. The three-band Hubbard model with an on-site Cu Coulomb interaction U_d, which is large compared to the difference in energy ε between the O and Cu sites, provides a basic model for such a system. We have carried out Lanczos and Monte Carlo studies of a CuO_2 lattice described by a three-band Hubbard model. For U_d large compared with ε, and ε comparable to or larger than the bandwidth of the lower hole band, we find strong antiferromagnetic correlations and evidence for a charge-transfer gap at a filling of one hole per Cu. The antiferromagnetic correlations decrease with either hole or electron doping, and we see that the additional holes go primarily on the O sites, while additional electrons go onto the Cu sites. For large values of the intersite Cu-O Coulomb interaction V, the hole-doped system exhibits a charge-transfer instability. As V is reduced, this is reflected as a peak in the charge-transfer susceptibility near $\varepsilon+2V\approx U_d$, which we find is washed out by the strong Cu-O hybridization at realistic values of V. Attractive pairing interactions are found in both the d-wave and extended s^*-wave channels near the antiferromagnetic boundary.

I. INTRODUCTION

In the search for the mechanism responsible for pairing in the high-T_c superconductors, interest has focused on the two-dimensional (2D) CuO_2 sheets. Viewing the regions separating the sheets as providing a charge reservoir for doping[1] and a medium for 3D coupling of the pair field, one is led to ask what property or properties of a CuO_2 sheet can lead to pairing. The strong 2D antiferromagnetic correlations observed for a filling of one hole per Cu raise the possibility that antiferromagnetic spin fluctuations provide the basic pairing mechanism. Indeed, various approaches based on a 2D Hubbard model support this view,[2-7] and numerical simulations have shown that near half-filling there is an attractive pairing interaction in the $d_{x^2-y^2}$ channel.[8] However, these simulations give no indication of the development of superconducting long-range order as T decreases.[9,10] In addition, the experimentally observed temperature dependence of the penetration depth[11] and the Knight shifts,[12] as well as recent angular-resolved photoemission measurements,[13] favor a nodeless gap. Now, as discussed by Emery[14] and Varma *et al.*,[15] the insulating state of the high-temperature superconducting oxides is most likely a charge-transfer insulator[16] in which the gap is set by the difference in energy between the Cu and O sites[17] rather than the larger on-site Cu Coulomb interaction. Thus, one is led to explore the effects of charge fluctuations which may enhance the s^* pairing interaction arising from spin fluctuations or alternately provide an independent s^* pairing mechanism.[18-29] A natural framework for treating both spin and charge fluctuations is provided by the three-band Hubbard model for a CuO_2 sheet.

The three-band Hubbard model we have studied has a hole Hamiltonian[14]

$$H=-t\sum_{\langle il\rangle,s}(d_{is}^{\dagger}p_{ls}+p_{ls}^{\dagger}d_{is})-\mu\sum_{is}n_{is}+(\varepsilon-\mu)\sum_{ls}n_{ls}+U_d\sum_{i}n_{i\uparrow}n_{i\downarrow}+U_p\sum_{l}n_{l\uparrow}n_{l\downarrow}+V\sum_{\langle il\rangle}n_i n_l\ . \tag{1}$$

Here $d_{is}^{\dagger}$ creates a $d_{x^2-y^2}$ hole of spin s at a Cu site i and $p_{ls}^{\dagger}$ creates a p-σ hole of spin s at an O site l. The parameter ε sets the relative energy difference between the O and Cu sites, and t is the Cu-O one-electron overlap. Here we have neglected the oxygen-oxygen one-electron transfer and selected phase factors so that all the Cu-O overlaps have the same sign. The onsite Cu and O Coulomb energies are U_d and U_p, respectively, and V is the Cu-O intersite Coulomb interaction. Experimentally an insulating antiferromagnetic state occurs when the CuO_2 layer has one hole per Cu. As discussed by Zaanen *et al.*,[16] for large values of ε, the gap for the insulating state is a Mott-Hubbard gap which depends upon U_d. If, instead, $U_d>\varepsilon+2V$, the gap in the insulating state is a charge-transfer gap which depends upon ε and V. Here we are interested in exploring this latter regime. Some initial results from this study were presented in Ref. 25.

 ©1991 The American Physical Society

We will measure energy in units of t and set $U_p=0$ throughout. We will also initially set the intersite Coulomb interaction $V=0$. Then, in the large U_d regime, the behavior of the system is determined by the charge-transfer energy ε. The bandwidth W of the lowest band is

$$W=\left[\left[\frac{\varepsilon}{2}\right]^2+8\right]^{1/2}-\frac{\varepsilon}{2} \tag{2}$$

so that, for $U_d>\varepsilon>2$, the charge-transfer energy exceeds W and is less than U_d. In this region, the insulating state is characterized by a charge-transfer gap. In this case, when the system is doped away from one hole per Cu, the hole occupation of the Cu and O sites behaves in the characteristic manner illustrated in Fig. 1. Figures 1(a) and 1(b) show the hole occupation of the Cu and O sites versus the hole filling $n=\langle n_d+2n_p\rangle$ for $U_d=6$ and 12 with $\varepsilon=2$. These results were obtained for a 2×2 CuO_2 lattice using a Lanczos procedure. Figure 1(c) shows Monte Carlo results for a 4×4 CuO_2 lattice with $U_d=6$, $\beta=8$, and $\varepsilon=2$. One clearly sees that as additional holes are added to the $n=1$ system, they go largely onto the O sites. However, when electrons are added and n is decreased, the holes are removed from the Cu sites. By contrast, in the Mott-Hubbard limit, where ε is large, the oxygen occupancy remains uniformly small and the occupancy of the Cu site varies with n for both electron and hole doping. This is illustrated in Fig. 1(d), which shows data for $U_d=6$, $\varepsilon=8$ for a 2×2 lattice.

In the following sections we will continue to give results obtained from both Lanczos diagonalization of a 2×2 CuO_2 periodic cluster and Monte Carlo simulations[30] of a 4×4 CuO_2 periodic cluster. The Lanczos results give ground-state expectation values, while the Monte Carlo simulations are for finite temperature. In general, the fermion determinantal sign problem[30] limits the inverse temperature $\beta=t/T$ that can be achieved in the Monte Carlo simulations. Near a filling of one hole per CuO_2 unit, with $V=0$, β values of the order of 20 can be reached, while at fillings away from one hole per CuO_2 or for $V\neq0$, the sign problem limits β to less than of order 10. In this temperature range, the magnetic correlations are beginning to develop, but one is still well above the superconducting transition temperature. In addition, the zero-temperature superconducting correlation length is of order the linear dimension of a 4×4 CuO_2 lattice. Thus, we do not expect to see strong pairing correlations. However, just as the effective attractive electron-electron interaction mediated by phonons is well formed at temperatures below the lattice melting temperature, we expect that, when the system is cold compared to the characteristic superexchange or charge-transfer energies, it may be possible to determine whether there is an attractive or repulsive interaction in a given pairing channel.

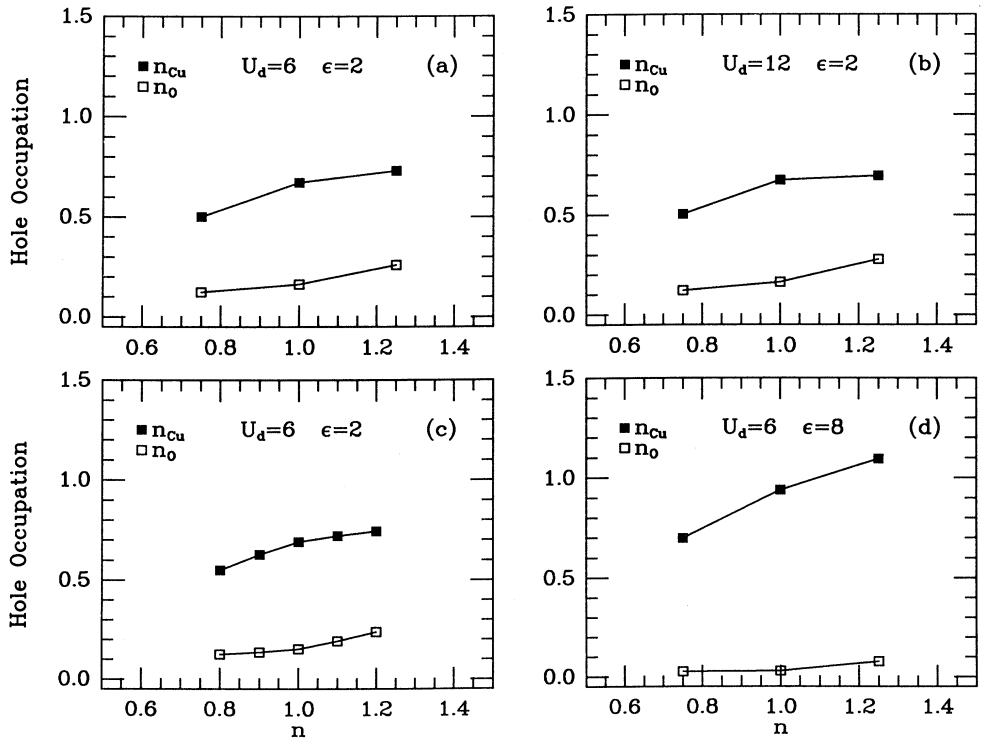

FIG. 1. Hole occupation of the Cu and O sites vs doping $n=\langle n_{Cu}+2n_O\rangle$ for different values of U_d and ε. In the charge-transfer regime (a)–(c), added holes tend to go onto the O sites, while added electrons go onto the Cu sites. In the Mott-Hubbard regime (d) the doping occurs primarily on the Cu site.

The properties of the $\varepsilon \gg U_d$ regime, where the oxygen orbital occupation is small, are expected to be similar to those of the single-band model. Therefore, we will focus both on an intermediate set of parameters, $U_d=4$, $\varepsilon=3$, and also on values $U_d=6$, $\varepsilon=2$, where charge-transfer fluctuations should be quite pronounced.

In Sec. II we begin by examining the formation of local moments and their correlations as seen in the magnetic structure factor. Here both the effect of doping and the dependence on ε, U_d, and V are of interest. Related Monte Carlo calculations have been carried out by Dopf, *et al.*[26,27] In Sec. II we also study the charge distribution on the CuO_2 lattice and the charge-transfer susceptibility. Weak-coupling calculations[23,24] as well as strong-coupling expansions[28,29] and cluster calculations[19–22] suggest that, when the system is doped sufficiently far away from the insulating state and the intersite Coulomb interaction is large, there can be a charge-transfer instability. This effect has also been seen in Gutzwiller variational calculations.[31] The 2×2 Lanczos calculations suggest that the system should have a charge-transfer instability for large values of V. However, for physical values $V<t$, we find that it is suppressed by the Cu-O hybridization.

Section III contains results for the pair field susceptibility which provides evidence for an attractive pairing interaction in both the $d_{x^2-y^2}$ and extended s^* channels. This is different from what was found for the single-band 2D Hubbard model[8] where only the $d_{x^2-y^2}$ channel showed a significant attraction. We find that this attraction occurs near the antiferromagnetic boundary. Section IV contains some concluding remarks.

II. MAGNETIC AND CHARGE CORRELATIONS

The local moment that develops on the Cu depends upon U_d, ε, V, and the filling n. For $n=1$ and $\varepsilon=3$, Fig. 2 shows Monte Carlo results on a 4×4 CuO_2 lattice at $\beta=6$ for the square of the local Cu moment

$$m_z(i)=d_{i\uparrow}^{\dagger}d_{i\uparrow}-d_{i\downarrow}^{\dagger}d_{i\downarrow}$$

versus U_d. Just as for the single-band 2D Hubbard model, a local moment develops as U_d increases.[32,33] However, for the CuO_2 three-band Hubbard model, the development of the Cu local moment also depends upon ε. Fig-

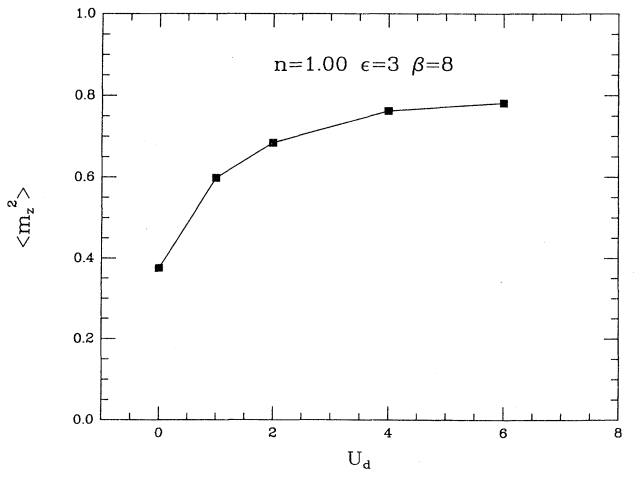

FIG. 2. The Cu local moment $\langle m_z^2 \rangle$ vs U_d. Results from a Monte Carlo simulation on a 4×4 CuO_2 lattice. The error bars are of order the size of the points.

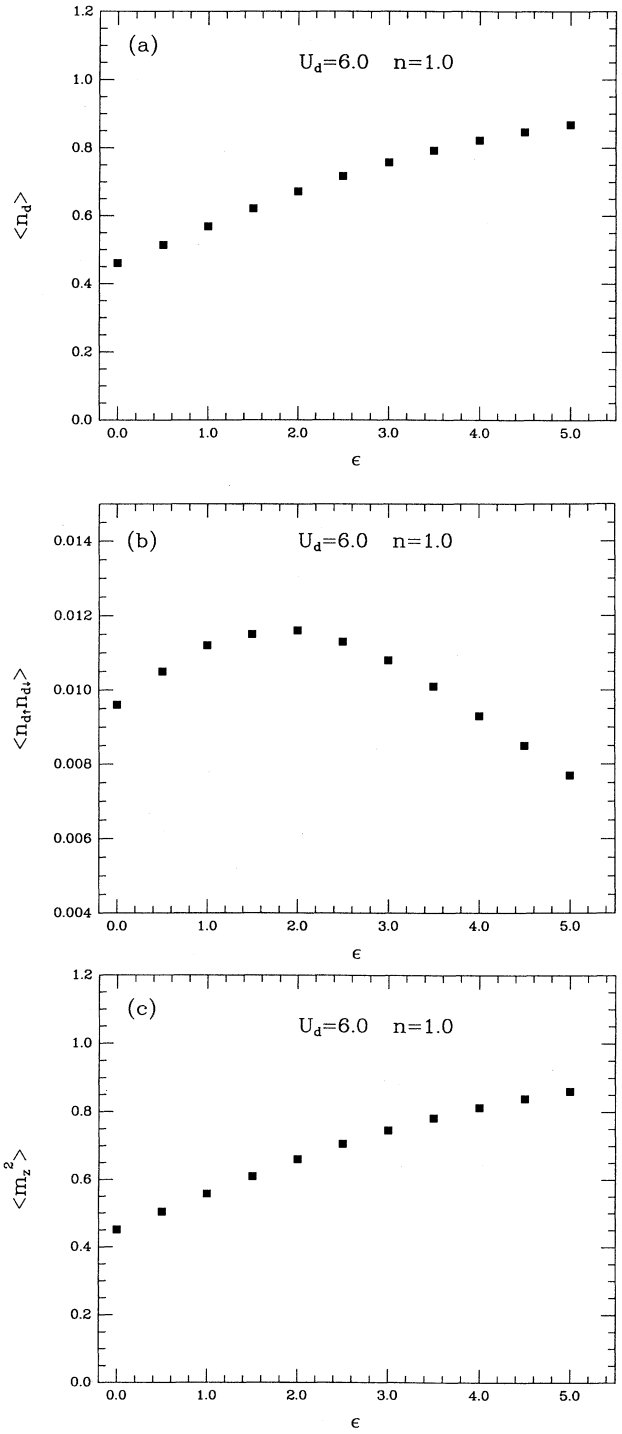

FIG. 3. (a) $\langle n_d \rangle$ vs ε, (b) $\langle n_{d\uparrow}n_{d\downarrow} \rangle$ vs ε, and (c) $\langle m_z^2 \rangle$ vs ε for $U_d=6$ and $\langle n \rangle=1$.

ure 2 displays results for $\varepsilon=3$, intermediate between the extreme cases of Fig. 1 where, for small ε, doped holes largely occupy the oxygen sites, and for large ε, the copper sites. For $\varepsilon=2$, $\langle M_{dz}^2 \rangle$ instead saturates at the lower value of 0.7, reflecting the increased delocalization of charge onto the oxygen sites as ε decreases. Figures 3(a) and 3(b) show $\langle n_d \rangle$ and $\langle n_{d\uparrow} n_{d\downarrow} \rangle$ versus ε for a 2×2 CuO_2 cluster with $n=1$, $\beta=8$, and $U_d=6$. The resulting Cu local moment

$$m_z^2=\langle n_{d\uparrow}+n_{d\downarrow}-2n_{d\uparrow}n_{d\downarrow} \rangle$$

is plotted in Fig. 3(c). Here, as ε increases, the holes move from the O to the Cu sites and $\langle n_d \rangle$ increases as expected. The nonmonotonic behavior of $\langle n_{d\uparrow} n_{d\downarrow} \rangle$ arises because the effective bandwidth $t_{\text{eff}}=t^2/\varepsilon$ is reduced as ε increases. This means that U_d/t_{eff} increases as ε increases, and the resulting correlations actually reduce $\langle n_{d\uparrow} n_{d\downarrow} \rangle$ even though $\langle n_{d\uparrow}+n_{d\downarrow} \rangle$ is increasing. The combined effect of this for $n=1$ is to increase the local moment as ε becomes larger than W, Eq. (2).

For $U_d=6$, $V=0$, and $\varepsilon=2$, adding one hole per four CuO_2 units ($n=1.25$) changes the rms value of the Cu moment from 0.805 to 0.806, while increasing the charge on O_2 by 0.19 out of the total of 0.25. Similarly, for $\varepsilon=4$, the rms value of the Cu moment changes only from 0.830 to 0.800 while the charge on O_2 in a CuO_2 unit increases by 0.17. Thus, in the charge-transfer parameter regime, where $U_d>\varepsilon>W$, the local Cu moment is relatively insensitive to doping and the majority of the added holes (of order 70–75 %) go onto the O sites as previously seen in Fig. 1. It is important to keep in mind that there are two O sites per unit cell so that, for example, when 70% of the added holes go onto the O sites, this means 35% on each O and 30% on the Cu.

The moments which form on the Cu are exchange coupled by a superexchange interaction mediated through the O sites. Figure 4 shows Monte Carlo results for the antiferromagnetic structure factor

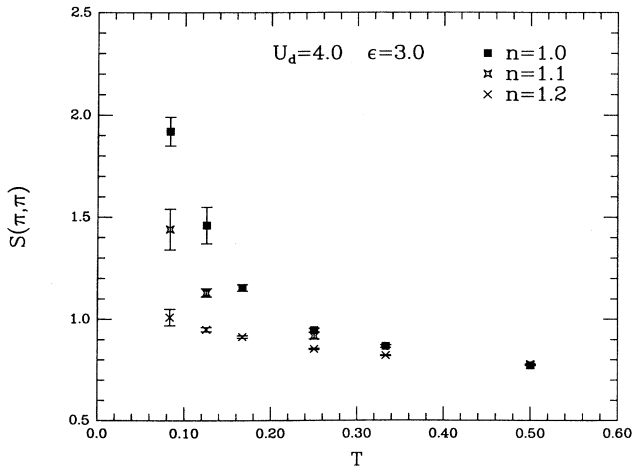

FIG. 4. The antiferromagnetic structure factor $S(\pi,\pi)$ vs temperature for different hole doping. This is Monte Carlo data on a 4×4 CuO_2 lattice, with $U_d=4$, $\varepsilon=3$, and various values of n.

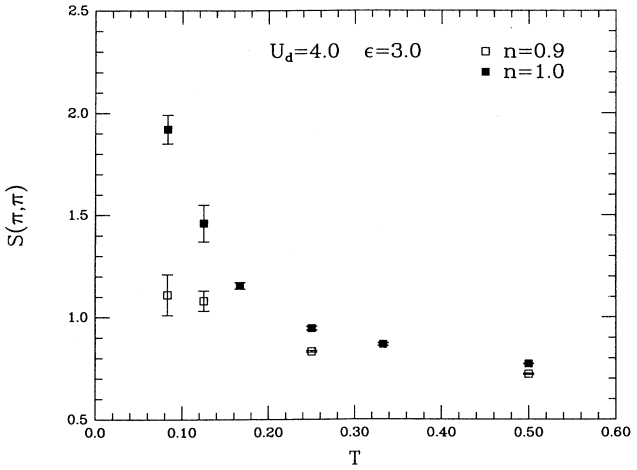

FIG. 5. $S(\pi,\pi)$ vs T for $n=1$ compared with an electron-doped system with $n=0.9$.

$$S(\pi,\pi)=\frac{1}{N}\sum_{i,j}\langle m_z(i)m_z(i+j)\rangle(-1)^j \tag{3}$$

versus temperature for a 4×4 CuO_2 lattice with the intermediate values $U_d=4$, $\varepsilon=3$, and various band fillings n. For $n=1$, $S(\pi,\pi)$ increases at low temperatures in a similar manner to its behavior for the half-filled Hubbard model,[32,33] which is consistent with the $n=1$ system having an antiferromagnetic ground state. As the system is doped away from $n=1$ by adding holes, $S(\pi,\pi)$ is suppressed. Figure 5 shows how $S(\pi,\pi)$ is changed by electron doping. We find that, if $S(\pi,\pi)$ is normalized by the square of the Cu moment $\langle m_z^2(i) \rangle$, the response to electron and hole doping is nearly symmetric. Meanwhile, as the system moves into the charge-transfer regime, the antiferromagnetic response is suppressed. This is illustrated in Fig. 6, where we show the variation of the magnetic structure factor $S(\pi,\pi)$ with doping for various

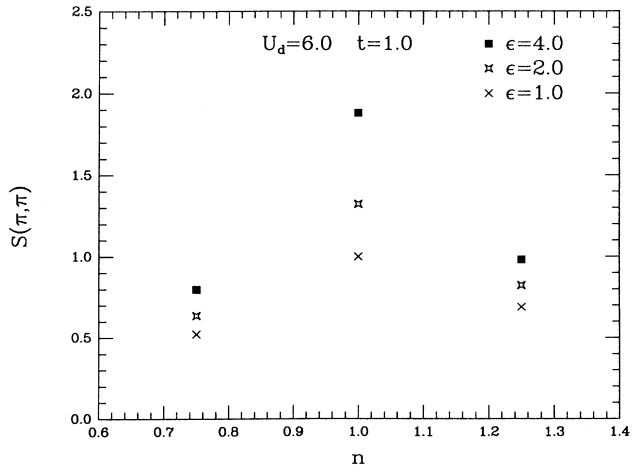

FIG. 6. Variation of $S(\pi,\pi)$ with doping for different values of ε. Here $U_d=6$, and these results are for a 2×2 CuO_2 lattice.

values of ε and $U_d=6$. These results, obtained from the 2×2 CuO_2 lattice, represent ground-state expectation values. The effect of decreasing ε is to move the $n=1$ system into the charge-transfer insulating regime.[25–27] As shown in Fig. 7, the local moment on the Cu increases with ε. At the same time, in the strong-coupling regime, the exchange interaction

$$J=\frac{4t^4}{\varepsilon^2}\left[\frac{1}{U_d}+\frac{1}{\varepsilon}\right]$$

decreases as ε is increased. Thus, at a fixed temperature and filling, $S(\pi,\pi)$ can exhibit a nonmonotonic variation with ε as shown in Fig. 7. Here $S(\pi,\pi)$ for $\beta=8$ initially increases as ε increases due to the increase in $\langle m_z^2\rangle$ and then decreases at larger ε due to the decrease in the exchange interaction. The full dependence of $\langle m_{dz}^2\rangle$ on U_d, ε, and T is an issue which deserves further attention.

We have seen that, in the three-band model, charge transfer to the oxygen sites reduces the copper moments. An alternate mechanism for the destruction of the antiferromagnetic order is the tendency of neighboring copper and oxygen spins to antialign, leading to a screening of the copper moments.[29] Additionally, a frustration of the copper antiferromagnetism can occur through the introduction of ferromagnetic tendencies on copper-copper links on which the intermediate oxygen is occupied.[34] The copper-oxygen antialignment which drives both these effects is clearly seen in the simulations and is certainly playing some role in the reduction of $S(\pi,\pi)$. Turning on the oxygen Coulomb repulsion, U_p is probably important to a full understanding of the system when oxygen occupation becomes large.

In these simulations, runs were carried out for various values of the chemical potential in order to study different band fillings. As previously discussed for the Hubbard model,[33] at low temperatures $\partial n/\partial\mu$ vanishes

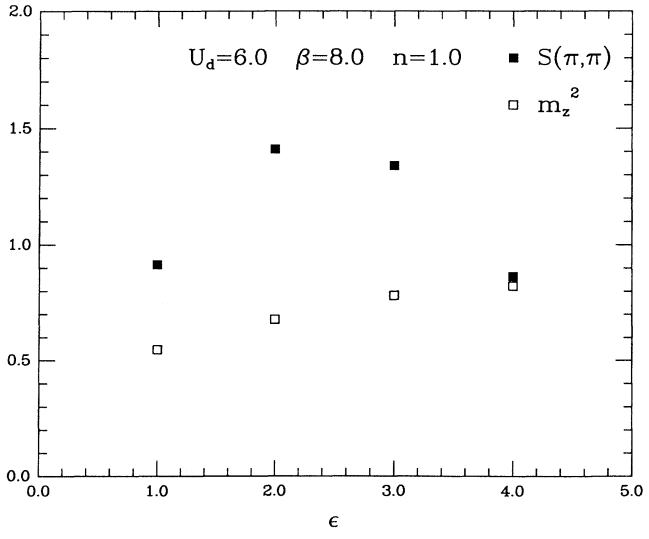

FIG. 7. $\langle m_z^2\rangle$ and $S(\pi,\pi)$ vs ε for a 4×4 CuO_2 lattice with $U_d=6$, $\beta=8$, and $n=1$.

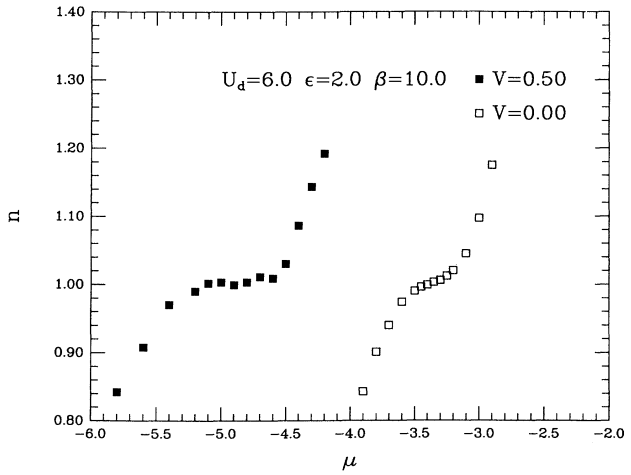

FIG. 8. Monte Carlo data for the band filling n vs μ on a 4×4 CuO_2 lattice. Here $\beta=10$, $U_d=6$, $\varepsilon=2$, and $V=0$ and 0.5. The effect of V is to enhance the charge-transfer gap.

when $n=1$ over a range of chemical potential set by the Mott-Hubbard gap. In the present case, a similar behavior has been reported by Dopf *et al.*[27] In Fig. 8, we plot Monte Carlo results on a 4×4 CuO_2 lattice for $\langle n\rangle$ versus μ. The parameters $U_d=6$, $\varepsilon=2$ place the system in the charge-transfer regime where a simple estimate of the gap would be $\varepsilon+2V$. One clearly sees that the Cu-O hybridization significantly reduces this estimate. However, V does enhance the gap as expected, although its effect is reduced by correlations.

Both the dependence of the gap on ε and V and the variation of the charge on the Cu and O sites shown in Fig. 1 differentiate the charge transfer from the Mott-Hubbard regime. In order to further explore the nature of the charge-transfer regime, we examine the charge-transfer fluctuations. A useful measure of these fluctuations is the charge-transfer susceptibility

$$\chi_{CT}(q)=\int_0^\beta d\tau\langle\bar{\rho}_q(\tau)\bar{\rho}_q^\dagger(0)\rangle \tag{4}$$

with $\bar{\rho}_q^\dagger$ the A_{1g} charge-transfer operator

$$\bar{\rho}_q^\dagger=\frac{1}{\sqrt{2N}}\sum_l e^{iq\cdot l}(n_l^d-n_l^{pa}-n_l^{pb}) . \tag{5}$$

Here n_l^d, n_l^{pa}, and n_l^{pb} are the charge-density operators on the Cu, x-axis O, and y-axis O of the lth CuO_2 unit cell, respectively. We are particularly interested in the $q\to0$ limit of χ_{CT} which determines the susceptibility of the system to a transfer of charge between the Cu and the O sites. It is straightforward to show that

$$\lim_{q\to0}\chi_{CT}(q)=\frac{\partial}{\partial\varepsilon}\langle n_d-2n_p\rangle . \tag{6}$$

Using a Lanczos procedure, we have calculated $\chi_{CT}(0)$ versus ε for $U_d=6$, and various values of V on a 2×2 CuO_2 lattice with three, four, and five holes corresponding to $n=0.75$, 1, and 1.25, respectively. Peaks in χ_{CT}

occur when charge shifts from the oxygen sites to the copper sites. These peaks are broadened by the Cu-O transfer t, so, in order to get a feeling for the behavior of χ_{CT} as ε is varied, we begin by showing, in Figs. 9(a)–(c), results with $t=0.25$. For $n=0.75$ and $n=1$, the charge-transfer susceptibility peaks at a small value of ε, shifted upwards by U_d times the probability of double occupancy of the Cu site. This peak reflects the mixed valence region in which the holes move from the oxygen to the copper sites. The area under χ_{CT} versus ε is set by $2n$, and as V increases, the maximum grows and the peak narrows. In the insulating antiferromagnetic phase with $n=1$ and $\varepsilon \gtrsim 2$, the charge-transfer susceptibility is small and the dominant fluctuations are associated with the spins. However, as shown in Fig. 9(c), the doped system with $n=1.25$ has both a mixed valence response near $\varepsilon \simeq 0$ and a charge-transfer structure for $\varepsilon \simeq U_d - 2V$.

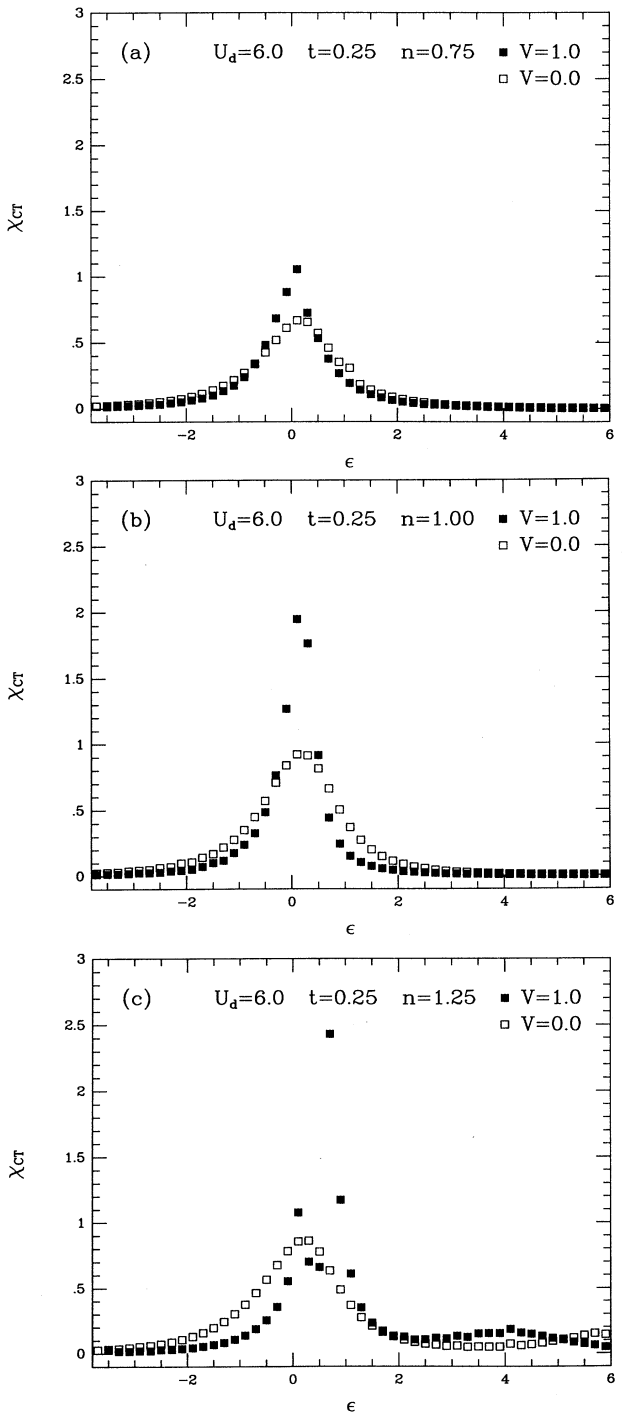

FIG. 9. The charge-transfer susceptibility χ_{CT} vs ε for different band fillings. (a) $n=0.75$, (b) $n=1.0$, and (c) $n=1.25$, with $t=0.25$, $U_d=6$, and $V=0$ and 1. These results were obtained from Lanczos calculation on a 2×2 CuO_2 lattice.

For $N+1$ holes on an N unit-cell cluster, a strong-coupling calculation predicts two peaks in the charge-transfer susceptibility at small ε. The first, at $\varepsilon=0$, describes the transition from a state of energy $(N+1)\varepsilon$ with all $N+1$ holes on the oxygen sites, to a state of energy $N\varepsilon$ having N oxygen holes and one copper hole with no neighboring oxygens occupied. The second transition at $\varepsilon=2V/(N-1)$ is to a state of energy $\varepsilon+2V$, where all but one of the holes are now on copper sites. In the thermodynamic $(N\rightarrow\infty)$ limit, these coalesce into a single peak but appear separated in Fig. 9(c) due to the finite lattice size. Of course, the final peak at $\varepsilon=U_d-2V$ in χ_{CT} is associated with the last remaining oxygen hole doubly occupying a copper site. This response appears in Fig. 9(c) as the broad peaks near $\varepsilon=4$ and 6 for $V=1$ and 0, respectively. The width of these peaks increases further with t so that the strong-coupling structure evident in Fig. 9(c) for $t=0.25$ is washed out as t increases. This is seen in Fig. 10 where we compare χ_{CT} versus ε for $n=1.25$ with $U_d=6$, $V=1$, and $t=0.250$ and 1.00. Monte Carlo results for χ_{CT} on a 4×4 CuO_2 lattice with $t=1$ and $n=1$ are shown in Fig. 11. Here the broadening produced by the larger copper-oxygen transfer t is again clearly evident. A similar broadening is observed at $n=1.25$, where χ_{CT} exhibits a single broad structureless peak centered at small ε. For an intersite Coulomb

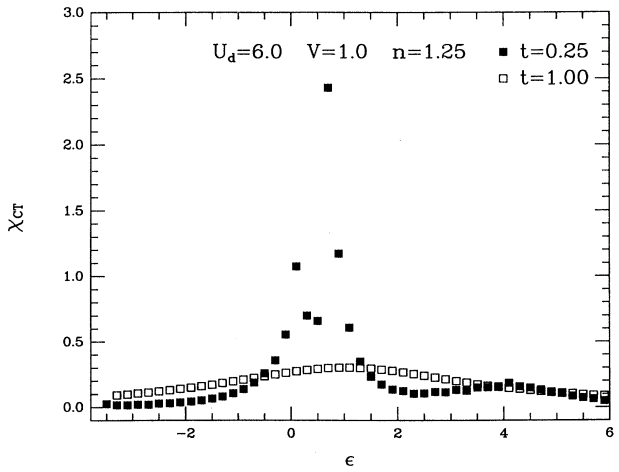

FIG. 10. The charge-transfer susceptibility χ_{CT} vs ε for $n=1.25$ with $U_d=6$, $V=1$, $t=0.25$ and 1.0. This clearly shows how increasing t broadens the response.

interaction $V<t$, the charge-transfer response near $\varepsilon=U_d-2V$ remains featureless, just as shown in Fig. 10 for the 2×2 CuO_2 lattice with $t=1$.

III. PAIRING INTERACTION

In the previous section, we have seen how the parameters ε, V, U_d, and the doping n affect the magnetic and charge correlations. In this section we discuss the possible role of the antiferromagnetic and charge-transfer fluctuations in providing an attractive pairing interaction. In analogy with the electron-phonon interaction, the exchange of antiferromagnetic fluctuations within a simple random-phase approximation (RPA) treatment have been shown to lead to an attractive interaction in the d-wave channel.[3,23,24] In the same way, weak-coupling calculations[23,24] near the charge-transfer instability have shown that the exchange of A_{1g} charge-transfer fluctuations can lead to an attraction in the s^* channel. However, from these calculations it appears that the system must be doped a significant amount away from $n=1$ and V must be larger than t for the charge-transfer fluctuations to provide an attraction. On the other hand, Emery and Reiter[18] have suggested that a modest value of V can enhance the spin-fluctuation mechanism, giving rise to an increase in the effective superexchange coupling between two Cu's in the presence of doped holes. They point out that this can lead to an s^*-channel attraction. Alternately, Wagner *et al.*[29] have argued that V can lead to an enhancement of the Kondo Cu-O interaction and via a constructive interplay with the Cu-Cu antiferromagnetic exchange to an s^*-wave attraction which exceeds the d-wave attraction for a range of doping near $n=1$.

Lanczos calculations have also been used to study the binding of two holes on small CuO_2 clusters.[19–22] Here magnetic, charge-transfer, and combined mechanisms were identified in various parameter regimes. However, for the small clusters that could be diagonalized, the negative binding energies for $V=0$, which arose from spin-spin correlations, disappeared when physically reasonable on-site oxygen Coulomb interactions were taken into account. In addition, it was found that unphysically large values of V were required to obtain negative binding energies in the charge-transfer regime. Furthermore, this pushed the system very near to a charge-transfer instability.

For example, in Ref. 19 it was found that, for $U_d=8$ and $\varepsilon=1$, the binding energy

$$\Delta=E(6)+E(4)-2E(5)$$

for two holes added to a 2×2 CuO_2 cluster was initially reduced by V, but for $V>1.5$, Δ became negative. Then, as V approached 2, the system became unstable with respect to a real-space condensation of holes. Following this procedure we have calculated the binding energy Δ for $U_d=6$, $V=1$, and various values of t. In Fig. 12, Δ is plotted versus ε for $U_d=6$, $V=1$, and $t=0.50$ and 1.00. One sees that, for $t=0.50$, there is a region of binding near the $\varepsilon=0$ peak in the charge-transfer susceptibility, but there is no region of binding for $t=1.00$. Naturally, since the energies are measured in units of t, the $t=0.50$ curve corresponds to an effective set of parameters, "$t=1$, $U_d=12$, $V=2$." Thus, it appears that one needs $V>t$ in order to obtain this type of binding due to charge-transfer fluctuations. Large values of V/t are accessible to Lanczos studies, but not to the quantum Monte Carlo where the fermion sign problem prevents simulations at low temperature. It is also interesting that the binding occurs near the $\varepsilon\cong0$ peak rather than near the $\varepsilon\cong U_d-2V$ regime.

An alternative approach to examine the tendency towards pairing is to calculate various pair-field susceptibilities. The pair-field susceptibility for the α-singlet channel is given by

$$P_\alpha=\int_0^\beta d\tau\langle\Delta_\alpha(\tau)\Delta_\alpha^\dagger(0)\rangle \tag{7}$$

with

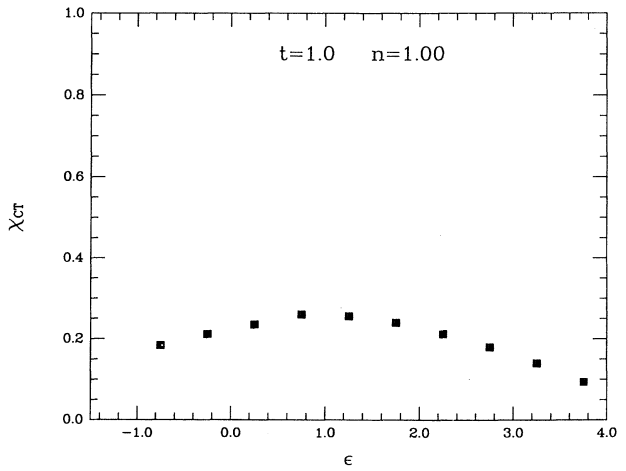

FIG. 11. χ_{CT} vs ε for a 4×4 CuO_2 lattice at $\beta=8$ with $t=1$, $V=0$, and $n=1$.

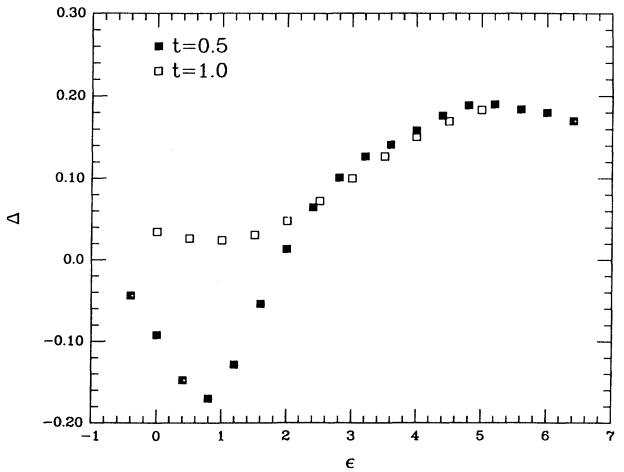

FIG. 12. The binding energy Δ for adding two holes to a 2×2 CuO_2 cluster vs ε for $U_d=6$, $V=1$, and $t=0.5$ and 1.0.

$$\Delta_\alpha^\dagger = \frac{1}{\sqrt{N}} \sum_p g_\alpha(p) d_{p\uparrow} d_{-p\downarrow} \ . \tag{8}$$

Here $g_\alpha(p)=1$ for s wave and $\cos p_x \pm \cos p_y$ with the plus sign for an extended s^* wave and the minus sign for d wave, respectively. By using the Cu d operators, we are assuming, consistent with NMR data,[12] that the pair field has some overlap with the Cu sites. In order to determine whether the interaction is attractive or repulsive in a given channel, we also calculate $\bar{P}_\alpha$, given by

$$\bar{P}_\alpha = \int_0^\beta d\tau \frac{1}{N} \sum_p G_{p\uparrow}(\tau) G_{-p\downarrow}(\tau) g_\alpha^2(p) \ , \tag{9}$$

with G_{ps} the dressed single-particle propagator. As discussed in Ref. 8, the quantity $\bar{P}_\alpha$ gives the contribution to the pair-field susceptibility, which comes from two dressed, but noninteracting, propagators. Thus, $P_\alpha - \bar{P}_\alpha$ represents the contribution of the particle-particle interactions in the αth channel and is positive for an attractive interaction and negative for a repulsive interaction. As discussed in the Introduction, we expect that, although it may not be feasible to carry out Monte Carlo simulations at the low temperatures required to see a strong buildup of pairing correlations, we should be able to reach temperatures which are sufficiently low that the fluctuations which mediate the pairing are well formed.

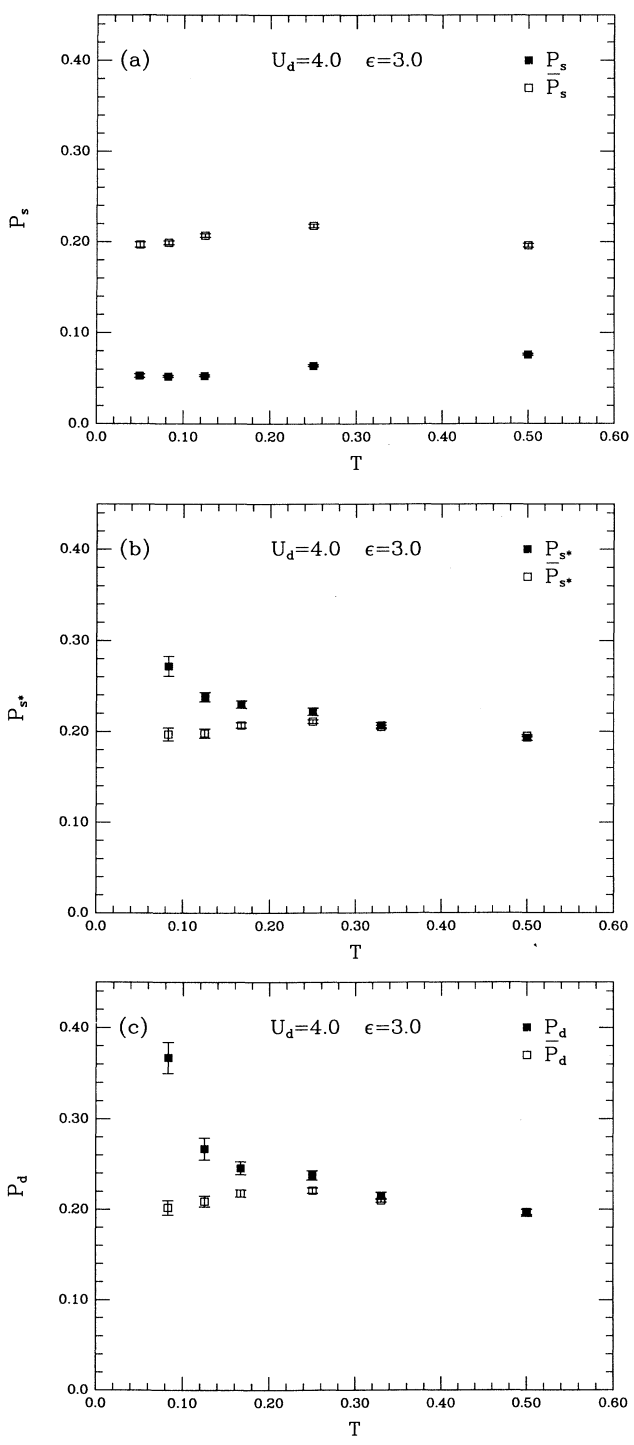

FIG. 13. The temperature dependence of the pair-field susceptibilities P_α and $\bar{P}_\alpha$ for $U_d=4$, $\varepsilon=3$, and $n=1$. (a) s wave, (b) s^* wave, and (c) d wave.

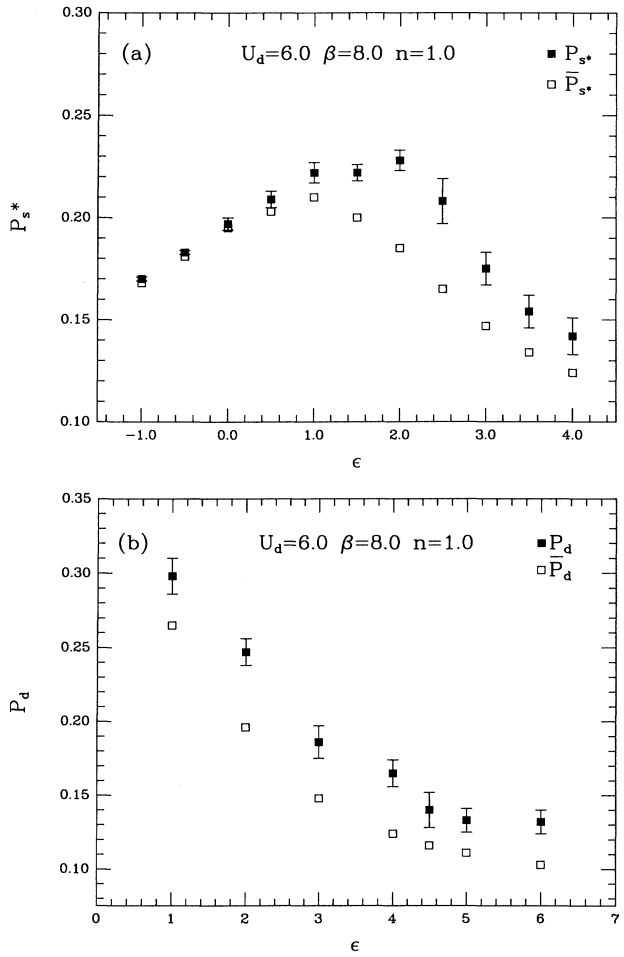

FIG. 14. P_α and $\bar{P}_\alpha$ vs ε with $n=1$, $U_d=6$, and $\beta=8$. (a) s^* wave and (b) d wave.

An example of the temperature dependence of the pair-field susceptibilities is shown in Figs. 13(a)–13(c). Here, for intermediate values of the parameters $U_d=4$, $\varepsilon=3$, $V=0$, and $n=1$, we have plotted P_α and $\bar{P}_\alpha$ for the s-, s^*-, and d-wave channels. It is clear that the interaction is repulsive in the s-wave channel. Note that this repulsive behavior is evident even for temperature $T\sim 1$. This reflects the on-site U_d interaction. Since this static interaction exists at all temperatures, the suppression of P_s relative to $\bar{P}_s$ extends over the full temperature range. Figures 13(b) and 13(c) show results for the extended s^*- and d-wave channels, respectively. Here we see a quite different behavior. First, at high temperatures where spin correlations are negligible, P_α is equal to $\bar{P}_\alpha$. As the temperature is lowered and the antiferromagnetic correlations form, P_α increases over $\bar{P}_\alpha$, indicating an attractive spin-fluctuation-mediated interaction for both the s^*- and d-wave channels. The d-wave channel appears to be the most attractive. We believe that the suppression of the noninteracting dressed propagator contributions to $\bar{P}_\alpha$ at low temperatures reflects the formation of a spin-density-wave gap in the quasiparticle spectrum for $n=1$. Similar behavior has been found for the half-filled Hubbard model,[8] although there only the d wave showed any significant enhancement from the interactions. One significant distinction between the single- and three-band models is this very marked increase in the enhancement of the extended s^*-wave pairing response. This enhancement of P_α over $\bar{P}_\alpha$ for the s^*- and d-wave responses depends upon ε as shown in Figs. 14(a) and 14(b). It appears to be associated with intermediate values of ε, where the charge-transfer insulating state has well-developed local moments which are strongly exchange coupled. At larger values of ε, the exchange coupling decreases. Thus, the ε dependence of this enhancement also supports identification of the antiferromagnetic spin fluctuations as the source of the pairing interaction.

Note that, although these results for the 4×4 CuO_2 lattice were taken with a chemical potential adjusted to give $n=1$, the addition of two holes by $\Delta_a^\dagger$ corresponds to a doping of $n=1.125$. We now explore the more general doping problem. In Figs. 15(a) and 15(b) the extend-

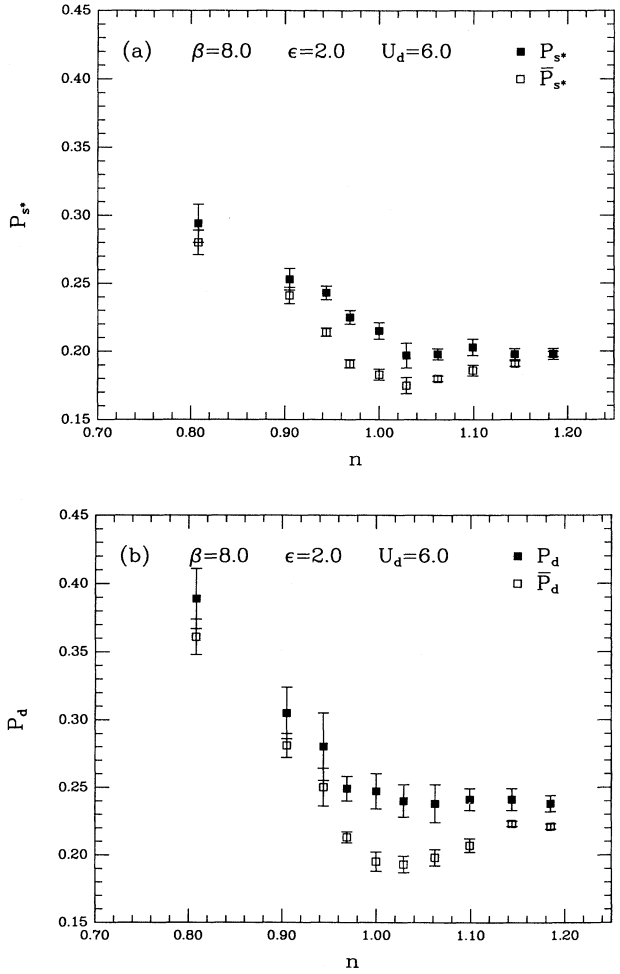

FIG. 15. The pair-field susceptibilities P_α and $\bar{P}_\alpha$ vs n for $U_d=6$, $\varepsilon=2$, and $\beta=8$. (a) s^* wave, and (b) d wave.

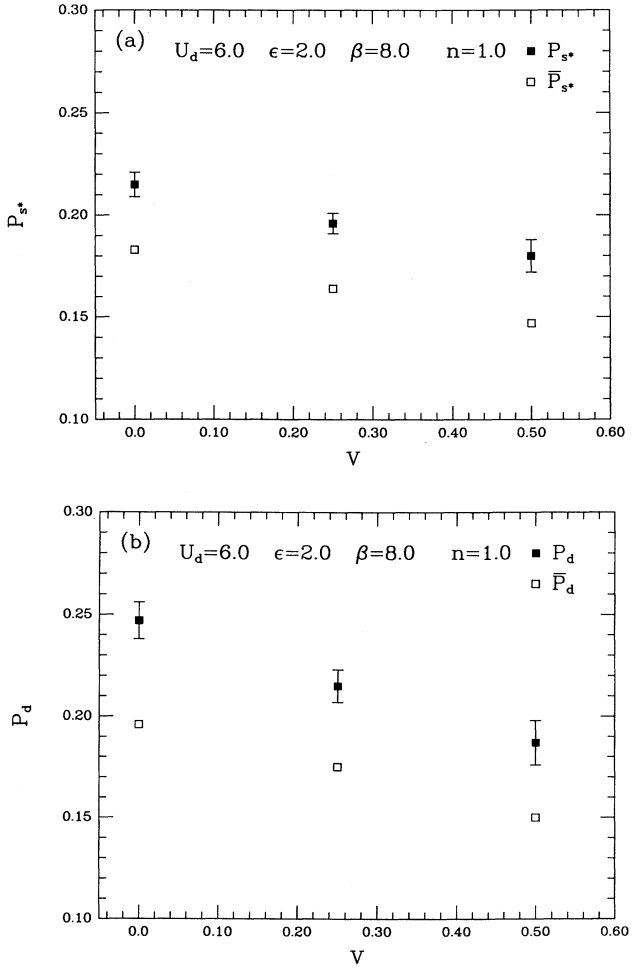

FIG. 16. The pair-field susceptibilities vs V for $U_d=6$, $\varepsilon=2$, and $\beta=8$. (a) s^* wave and (b) d wave.

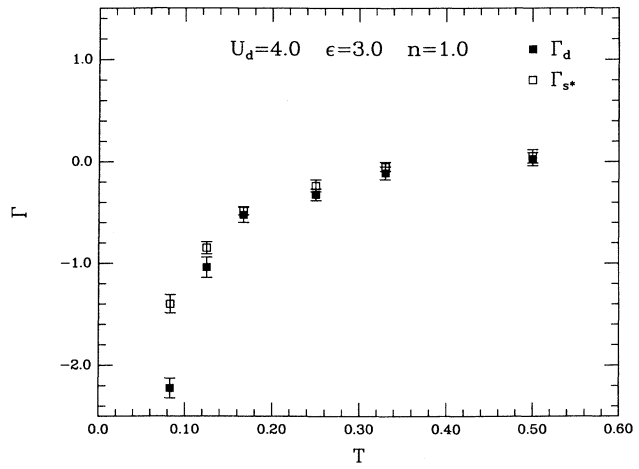

FIG. 17. Γ_α for the s^*- and d-wave channels vs T for $U_d=4$, $\varepsilon=3$, and $n=1$.

ed s^*- and d-wave pair-field susceptibilities P_α and $\bar{P}_\alpha$ are plotted versus n for $\beta=8$ with $U_d=6$, $V=0$, and $\varepsilon=2$. As discussed, the extended s^*-wave and d-wave channels have $P_\alpha > \bar{P}_\alpha$, indicating an attractive pairing interaction for n near 1. The d-wave susceptibilities are larger than the s^*-wave susceptibilities, but both are increased by the interaction. In all cases, the noninteracting dressed propagator response $\bar{P}_\alpha$ is depressed at $n=1$, reflecting the formation of a spin-density-wave gap in the quasiparticle spectrum at $n=1$. Near $n=1$ the enhancement due to the interaction vertex is most visible. However, based upon the behavior of $\bar{P}_\alpha$, the region most favorable to the formation of a superconducting phase in a large system is expected to occur as the system is doped away from $n=1$, and the gap in the quasiparticle spectrum disappears.

When the intersite Coulomb interaction V is turned on, the pair-field susceptibilities P_α and $\bar{P}_\alpha$ are both suppressed, as shown in Fig. 16. This is presumably associated with wave-function renormalization effects and makes it difficult to determine the effect of V on the pairing interaction. One approach to sorting out the wave-

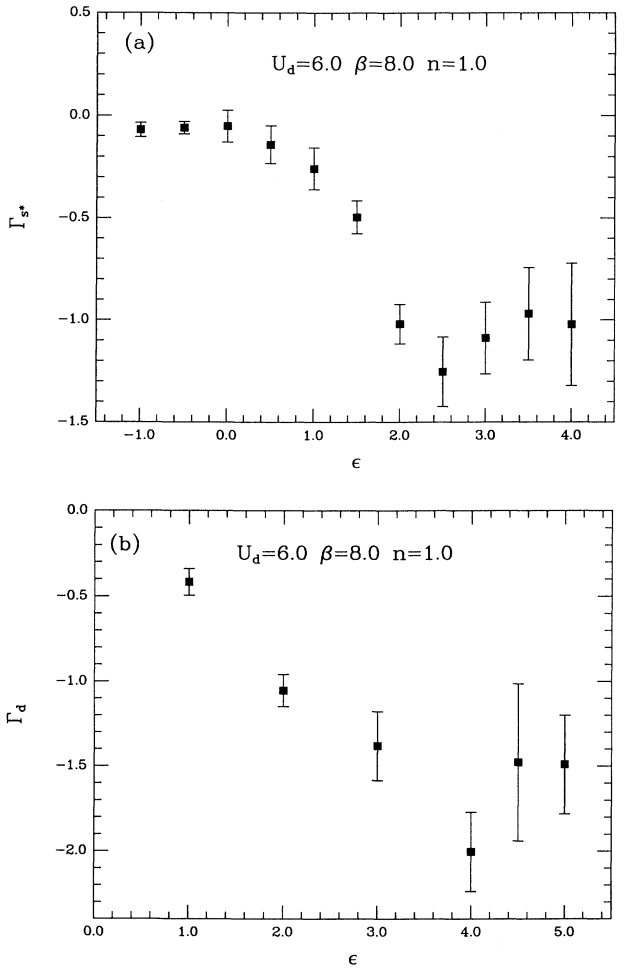

FIG. 18. Γ_α vs ε as determined using Eq. (9) and the results for P_α and $\bar{P}_\alpha$ shown in Fig. 14. (a) s^*-wave channel and (b) d-wave channel. Here $U_d=6$, $V=0$, $n=1$, and $\beta=8$.

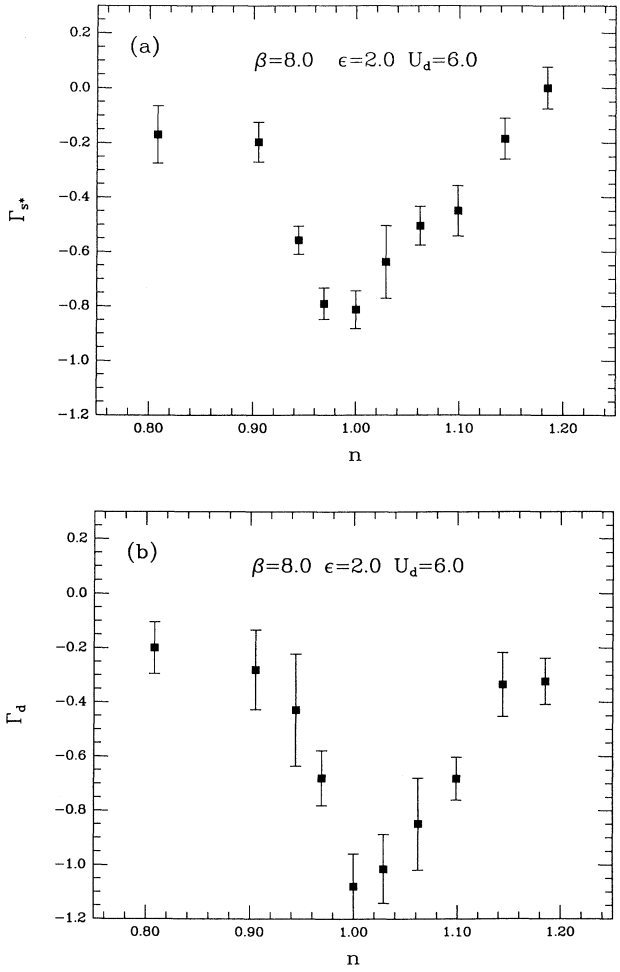

FIG. 19. Γ_α vs n with $U_d=6$, $V=0$, $\varepsilon=2$, and $\beta=8$. (a) s^*-wave channel and (b) d-wave channel.

function renormalization effects is to assume that the irreducible particle-particle interaction vertex is replaced by a constant Γ_α. Then

$$P_\alpha = \frac{\bar{P}_\alpha}{1+\Gamma_\alpha \bar{P}_\alpha} , \tag{10}$$

and solving for Γ_α, one obtains

$$\Gamma_\alpha = P_\alpha^{-1} - \bar{P}_\alpha^{-1} . \tag{11}$$

Figure 17 shows Γ_α for the s^*- and d-wave channels versus T for $U_d=4$, $\varepsilon=3$, and $n=1$ obtained from the results for P_α and $\bar{P}_\alpha$ shown in Figs. 13(b) and 13(c). As the temperature is lowered and the antiferromagnetic spin correlations develop, Γ_{s*} and Γ_d become attractive. As previously discussed, Γ_s is repulsive at all temperatures, reflecting the static on-site Cu Coulomb interaction U_d.

We have also used Eq. (11), with the results shown in Figs. 14 and 15, to determine the dependence of Γ_α on ε and n shown in Figs. 18 and 19, respectively. Comparing

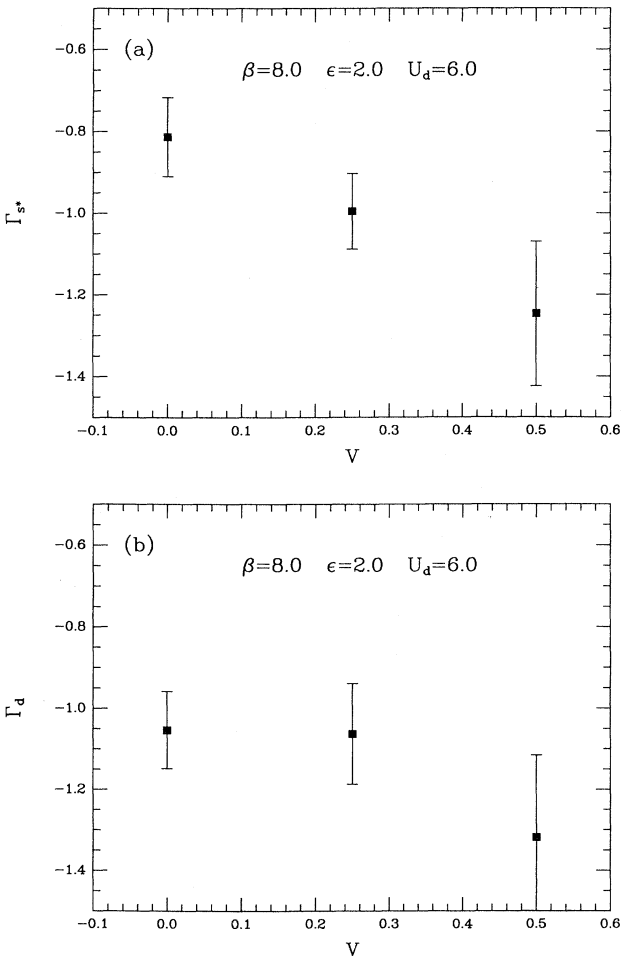

FIG. 20. Γ_α vs V with $U_d=6$, $\varepsilon=2$, $\beta=8$, and $n=1$. (a) s^*-wave channel and (b) d-wave channel.

Γ_α versus ε with the results for $S(\pi,\pi)$ versus ε in Fig. 7, it is clear that the strength of the antiferromagnetic spin fluctuations are correlated with the behavior of Γ_{s*} and Γ_d. This is also clear from its n dependence. Figure 20 shows Γ_α versus V for the d and s^* channels determined from the Monte Carlo data of Fig. 16. Plotted in this way, it appears that V enhances the Γ_{s*} attraction and perhaps also enhances Γ_{d*}. This implies that the decrease in P_{s*} and P_d seen in Figs. 16(a) and 16(b) as V is increased arises from wave-function renormalization effects.[35] The constant vertex approximation of Eq. (11) represents one approach to removing these effects and examining the dependence of the pairing interaction itself on V.

IV. CONCLUSIONS

The qualitative behavior of the spin and charge correlations of the three-band Hubbard model, discussed in Sec. II, are similar to the observed behavior of the cuprate materials. In particular, the dependence of the site occupancy with respect to electron and hole doping, the occurrence of a charge-transfer gap which depends upon ε and V, the strong antiferromagnetic correlations at a filling of one hole per Cu, along with the rapid decrease of these correlations with doping, all fit the basic experimental pattern which has emerged. Our parameters ($t=1$, $U_d=6$, $\varepsilon=2$, $V=0.5$) are in rough agreement[36] with various estimates ($t=1.5$, $U_d=9$, $\varepsilon=3$, $V=0.75$) which have been made, and we have varied them to include the $\varepsilon \sim U_d - 2V$ regime.[17]

In agreement with earlier cluster calculations and weak-coupling results, we find that unphysically large values of V are required to enter the region of the charge-transfer instability. In addition, as one expects, the charge-transfer susceptibility lacks the electron-hole-doping symmetry suggested by the La-Sr and Nd-Ce materials.

Near the antiferromagnetic regime, characterized by a doping of one hole per CuO_2, we find evidence for attractive interactions in both the s^*-wave and d-wave channels. This is different from the one-band Hubbard model where only the d-wave channel showed a significant attraction. It suggests that there is an attractive near-neighbor unit-cell interaction between two fermions. Replacing the irreducible particle-particle interaction vertex by a constant Γ_α, we used Monte Carlo data for the pair-field susceptibility to determine the dependence of Γ_α on ε, n, and V. The dependence of Γ_α on ε and n showed a strong correlation with the dependence of the antiferromagnetic response on these same parameters. It also appeared that, near the antiferromagnetic boundary, V enhanced the s^*-wave pairing interaction and possibly the d-wave one as well. From our present results we are unable to determine which channel, d or s^* wave, will dominate at low temperatures or, in fact, whether the system will ultimately go into a superconducting phase. Clearly one needs to extend these simulations to lower temperatures and larger lattices in order to further ex-

plore the pairing correlations of the three-band Hubbard model.

ACKNOWLEDGMENTS

We would like to acknowledge useful discussions with N. E. Bickers, E. Loh, Jr., S. Coppersmith, P. B. Littlewood, J. B. Torrance, W. Hanke, and C. M. Varma. We would also like to express our gratitude to the Department of Energy, who supported this work under a "Grand Challenge" computing grant and under grant No. DE-FG03-85ER45197. The computations were carried out on the NMFE Cray computers at Livermore National Laboratory.

[1]A. W. Sleight, Physica C **162**, 3 (1989).
[2]P. W. Anderson, Science **235**, 1196 (1987).
[3]N. E. Bickers, D. J. Scalapino, and R. T. Scalettar, Int. J. Mod. Phys. B **1**, 687 (1987).
[4]J. R. Schrieffer, S. G. Wen, and S. C. Zhang, Phys. Rev. Lett. **60**, 944 (1988); Phys. Rev. B **39**, 11 663 (1989).
[5]C. Gross, R. Joynt, and T. M. Rice, Z. Phys. B **68**, 425 (1987); C. Gross, Phys. Rev. B **38**, 931 (1988).
[6]N. E. Bickers, D. J. Scalapino, and S. R. White, Phys. Rev. Lett. **62**, 961 (1989).
[7]K. Yonemitsu, J. Phys. Soc. Jpn. **58**, 4576 (1989).
[8]S. R. White, D. J. Scalapino, R. L. Sugar, N. E. Bickers, and R. T. Scalettar, Phys. Rev. B **39**, 839 (1989).
[9]M. Imada, J. Phys. Soc. Jpn. **57**, 3128 (1988); M. Imada and Y. Hatsugai, *ibid.* **58**, 3752 (1989).
[10]A. Moreo and D. J. Scalapino, Phys. Rev. B **43**, 8211 (1991).
[11]L. Krusin-Elbaum *et al.*, Phys. Rev. Lett. **62**, 217 (1989); D. R. Harshman *et al.*, Phys. Rev. B **39**, 217 (1989).
[12]P. C. Hammel *et al.*, Phys. Rev. Lett. **63**, 1992 (1989); C. H. Pennington *et al.*, Phys. Rev. B **39**, 2902 (1989).
[13]C. G. Olson *et al.*, Physica C **162-164**, 1697 (1989); Science **245**, 731 (1989).
[14]V. J. Emery, Phys. Rev. Lett. **58**, 2794 (1987).
[15]C. M. Varma, S. Schmitt-Rink, and E. Abrahams, Solid State Commun. **62**, 681 (1987).
[16]J. Zaanen, G. A. Sawatzky, and J. W. Allen, Phys. Rev. Lett. **55**, 418 (1985); A. M. Olés and J. Zaanen, Phys. Rev. B **39**, 9175 (1989).
[17]J. B. Torrance and R. M. Metzger, Phys. Rev. Lett. **63**, 1515 (1989).
[18]V. J. Emery and G. Reiter, Phys. Rev. B **38**, 4547 (1988).
[19]J. E. Hirsch, S. Tang, E. Loh, Jr., and D. J. Scalapino, Phys. Rev. Lett. **60**, 1668 (1988); Phys. Rev. B **39**, 243 (1989).
[20]M. Ogata and H. Shiba, J. Phys. Soc. Jpn. **57**, 3074 (1988).
[21]C. A. Balseiro, A. G. Rojo, E. R. Gagliano, and B. Alascio, Phys. Rev. B **38**, 9315 (1988).
[22]W. H. Stephan, W. v. d. Linden, and P. Horsch, Phys. Rev. B **39**, 2924 (1989).
[23]P. B. Littlewood, C. M. Varma, S. Schmitt-Rink, and E. Abrahams, Phys. Rev. B **39**, 12 371 (1989).
[24]R. Putz, B. Ehlers, L. Lilly, A. Muramatsu, and W. Hanke, Phys. Rev. **41**, 853 (1990).
[25]R. T. Scalettar, Physica C **162**, 313 (1989).
[26]G. Dopf, A. Muramatsu, and W. Hanke, Physica C **162**, 807 (1989).
[27]G. Dopf, A. Muramatsu, and W. Hanke, Phys. Rev. B **41**, 9264 (1990); G. Dopf, T. Kraft, A. Muramatsu, and W. Hanke (unpublished).
[28]H.-B. Schüttler and A. J. Fedro, J. Less Common Met. **149**, 385 (1989); H.-B. Schüttler, Phys. Rev. B **38**, 2854 (1988).
[29]J. Wagner, A. Muramatsu, and W. Hanke, Phys. Rev. B **42**, 2200 (1990).
[30]The fermion Monte Carlo procedure we used in this work is described in S. R. White, D. J. Scalapino, R. L. Sugar, E. Y. Loh, Jr., J. E. Gubernatis, and R. T. Scalettar, Phys. Rev. B **40**, 506 (1989); and in E.Y. Loh, Jr., J. E. Gubernatis, R. T. Scalettar, S. R. White, D. J. Scalapino, Phys. Rev. B **41**, 9301 (1990).
[31]S. N. Coopersmith, Phys. Rev. B **39**, 9671 (1989); S. N. Coopersmith and P. Littlewood (unpublished).
[32]J. Hirsch, Phys. Rev. B **31**, 4403 (1985).
[33]A. Moreo, D. J. Scalapino, R. L. Sugar, S. R. White, and N. E. Bickers, Phys. Rev. B **41**, 2313 (1990).
[34]A. Aharony, R. J. Birgeneau, A. Coniglio, M. A. Kastner, and H. E. Stanley, Phys. Rev. Lett. **60**, 1330 (1988).
[35]Note that, even for the electron-phonon interaction, at high temperatures P_s is reduced as the electron-phonon coupling is turned on. This simply reflects self-energy effects which reduce the quasiparticle component of G. This wave-function renormalization effect can be seen by calculating P_s and P_{s*} within the Eliashberg theory, R. Scalettar, N. E. Bickers, and D. J. Scalapino, in *Computer Simulation Studies in Condensed Matter Physics,* Vol. 33 of *Springer Proceedings in Physics,* edited by D. P. Landau, K. K. Mon, and H.-B. Schüttler, (Springer-Verlag, Berlin, 1988), p. 166.
[36]A. K. McMahan, R. M. Martin, and S. Satpathy, Phys. Rev. B **38**, 6650 (1988); M. S. Hybertsen, M. Schlüter, and N. E. Christiansen, *ibid.* **39**, 9028 (1989). Note that, since our energy scale is set by t, the relevant comparison is U_d/t, ε/t, V/t, etc. We have neglected the one-electron oxygen-oxygen transfer and the on-site oxygen Coulomb interaction.